28. Young, R. A. (ed.) *The Rietveld Method* (Oxford Univ. Press, Oxford, 1993).
29. Larson, A. C. & von Dreele, R. B. *GSAS Report LAUR 86-784* (Los Alamos National Laboratory, 1986).
30. Breck, D. W. *Zeolite Molecular Sieves* (Wiley, New York, 1974).
31. Mitariten, M. & Dolan, W. Nitrogen removal from natural gas with molecular gate technology. *Proc. Laurance Reid Gas Cond. Conf.* **51,** 1–16 (2001).
32. Abrams, L. & Corbin, D. R. in *Topics in Inclusion Science* Vol. 6, *Inclusion Chemistry with Zeolites: Nanoscale Materials by Design* (eds Herron, N. & Corbin, D. R.) 4–6 (Kluwer, Dordrecht, 1995).

Supplementary information is available on *Nature*'s World-Wide Web site (http://www.nature.com) or as paper copy from the London editorial office of *Nature*.

Acknowledgements

We thank J. Curran for discussions and assistance in the preparation of the manuscript, and VTI Corp. for the data of Fig. 5. This work was supported by ATP/NIST, the David and Lucile Packard Foundation and NSF-CTS.

Correspondence and requests for materials should be addressed to S.M.K. (e-mail: steve.kuznicki@engelhard.com).

The timing of the last deglaciation in North Atlantic climate records

Claire Waelbroeck*, Jean-Claude Duplessy*, Elisabeth Michel*, Laurent Labeyrie*†, Didier Paillard* & Josette Duprat‡

** Laboratoire des Sciences du Climat et de l'Environnement, Domaine du CNRS, bât. 12, 91198 Gif-sur-Yvette, France*
† Département des Sciences de la Terre, Université Paris-sud Orsay, bât. 504, 91104 Orsay, France
‡ Département de Géologie et Océanographie, CNRS UMR 5805, Université de Bordeaux I, Talence, France

To determine the mechanisms governing the last deglaciation and the sequence of events that lead to deglaciation, it is important to obtain a temporal framework that applies to both continental and marine climate records. Radiocarbon dating has been widely used to derive calendar dates for marine sediments, but it rests on the assumption that the 'apparent age' of surface water (the age of surface water relative to the atmosphere) has remained constant over time[1,2]. Here we present new evidence for variation in the apparent age of surface water (or reservoir age) in the North Atlantic ocean north of 40° N over the past 20,000 years. In two cores we found apparent surface-water ages to be larger than those of today by 1,230 ± 600 and 1,940 ± 750 years at the end of the Heinrich 1 surge event (15,000 years BP) and by 820 ± 430 to 1,010 ± 340 years at the end of the Younger Dryas cold episode. During the warm Bølling–Allerød period, between these two periods of large reservoir ages, apparent surface-water ages were comparable to present values. Our results allow us to reconcile the chronologies from ice cores and the North Atlantic marine records over the entire deglaciation period. Moreover, the data imply that marine carbon dates from the North Atlantic north of 40° N will need to be corrected for these highly variable effects.

The last deglaciation is a period particularly well dated because it belongs to the time span covered by isotopic (^{14}C) dating techniques, which can be applied to both continental and marine sediments. Moreover, ^{14}C dates can be converted into calendar ages through calibration curves describing the variations in the atmospheric $^{14}C/^{12}C$ ratio over the past 20 kyr (ref. 3). Also, the uncertainty on the absolute dating by annual-layer counting of the Greenland ice cores is small (<550 yr) over the last 15 kyr (ref. 4). Therefore, it is possible to compare directly the timing of events from continental and ice-core records, and thus to infer causal mechanisms from the data. The situation is more complex for the marine data, as the ^{14}C dates are measured on foraminifera preserved in the sediments and hence reflect the $^{14}C/^{12}C$ ratio of the water in which the foraminifera calcified. The surface-water $^{14}C/^{12}C$ ratio is different from that of the contemporaneous atmosphere, reflecting the balance between the input of atmospheric ^{14}C and its removal by transport and radiodecay in the water column. This difference in $^{14}C/^{12}C$ ratio is usually expressed as the apparent or reservoir age of the water mass.

A compilation of pre-bomb surface-water ^{14}C content indicates that the modern surface reservoir age is about 400 ± 100 yr in the tropics and in the North Atlantic whereas it rises to 1,200 yr at higher latitudes in the Southern and North Pacific oceans[5,6]. Past reservoir ages most probably differed from those of today, but only sparse data exist. Reservoir ages have been measured in a few sites at given times in the past, by dating contemporaneous samples in marine sediments and in terrestrial organic matter, marked by the same volcanic ash layer[7–10].

Here, we present summer sea surface temperature (SST) reconstructions and benthic oxygen isotopic records ($\delta^{18}O_b$) from three sediment cores raised for the North Atlantic Ocean between 37 and 55° N (SU 81-18, 37° 46′ N, 10° 11′ W, 3,135 m; CH 69-09, 41° 45′ N, 47° 21′ W, 4,100 m; and NA 87-22, 55° 29′ N, 14° 41′ W, 2,161 m). These records have been dated by accelerator mass spectrometry on monospecific planktonic foraminifera samples[1,11,12] (see Supplementary Information Table 1). Radiocarbon ages have been converted into calendar ages with the CALIB 4.1 software[13], the smoothed (310-yr moving average) 1998 marine calibration curve

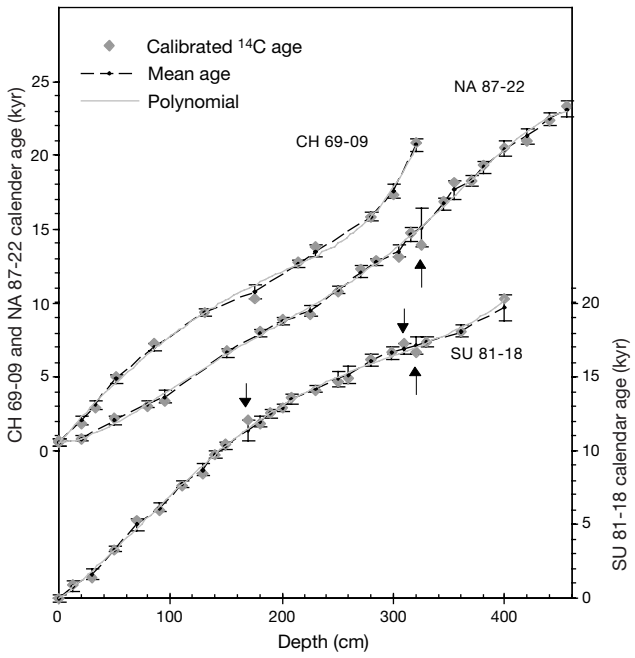

Figure 1 Age–depth relationships for the three North Atlantic deep sea cores. Calendar ages were calculated from the measured ^{14}C ages (see Supplementary Information Table 1) with the CALIB 4.1 software[13] and a constant surface reservoir age of 400 yr. For each core, two different interpolation schemes were used: first, we computed the fifth-order polynomial fitting the dated levels (grey line); second, we linearly interpolated the dated levels, leaving out one age in core NA 87-22 and three ages in core SU 81-18 that showed small age inversions (arrows). The error on the linearly interpolated age scale is taken as one standard deviation of the sample's calendar-age probability distribution given by CALIB 4.1. The error on the polynomial age scale is taken as the difference between the actual sample calendar age and the polynomial age computed at the same level, when this difference is larger than the error on the sample's calendar age. It is otherwise equal to the error on the linearly interpolated age scale. We derived the final age model for each core (black dots with 1-s.d. error bars) by taking the arithmetical mean of the above two timescales to ensure realistically large error bars. The final error estimate includes an additional 200-yr uncertainty, representing the maximum possible bioturbation bias. Both interpolation schemes support our conclusions.

of Stuiver *et al.*[3], and a constant surface reservoir age of 400 yr (Fig. 1). The method provides the probability distribution of the sample's calendar age.

The sedimentation rate is about 20 cm kyr^{-1} between 10 and 15 kyr before present (BP) for the three cores examined here (Fig. 1). Therefore, bioturbation should not induce significant biases[14]. Moreover, the ^{14}C ages were determined on planktonic monospecific samples selected in the species abundance maxima (see Supplementary Information Table 1), so that bioturbation distortion of the above dating is minimized.

The three North Atlantic SST series can now be plotted against calendar age, together with the GRIP or GISP2 ice–oxygen isotopic record, a proxy for air temperature[15] (Fig. 2). All three SST series depict a clear two-step warming of 7–12 °C amplitude from the end of the last glacial to the Holocene. The first warming phase is extremely abrupt, as can be seen in the two records of highest resolution (CH 69-09 and SU 81-18) and corresponds to GRIP's sharp increase in air temperature marking the transition between the last Heinrich event (H1) (ref. 16) and the Bølling–Allerød interval. Similarly, the second rapid-warming phase should correspond with the transition from the Younger Dryas cold episode to the Holocene.

Assuming a constant surface reservoir age implies very large leads of the SST increase at the two northernmost Atlantic sites with respect to the increase in air temperature above Greenland. These leads can be accurately evaluated (see Supplementary Information Table 2), with the total uncertainty on the warming-midpoint dates resulting from the error related to the time resolution and from the dating error (Fig. 1). The first sharp SST increase is found to lead the H1–Bølling–Allerød transition recorded in the Greenland ice by 1.94 ± 0.75 kyr in core NA 87-22, and by 1.23 ± 0.60 kyr in core CH 69-09. Similarly, the second abrupt SST increase leads the Younger Dryas–Holocene transition in the ice by 0.82 ± 0.43 kyr in core NA 87-22, and 1.01 ± 0.34 kyr in core CH 69-09. In contrast, the SST variations recorded in core SU 81-18, located further south (38° N), coincide with air temperature variations above Greenland.

Several lines of evidence drive us to conclude that the large leads observed in the northernmost records are not real climatic features. First, examining the marine $\delta^{18}O_b$ records reveals a similar significant lead of the decrease in $\delta_{18}O_b$ associated with the deglaciation in the northern records compared with the SU 81-18 mid-latitudes $\delta^{18}O_b$ record (Fig. 3a). The decrease in $\delta^{18}O_b$ taking place during deglaciations results from the combined effect of ice melting and deep-water warming. Because the three cores are geographically relatively close and bathed by water masses dominated by North Atlantic deep water (NADW), large changes in $\delta^{18}O_b$ should take place roughly simultaneously at the three locations. Therefore, a different timing of the warming cannot explain the lead of 1–2 kyr

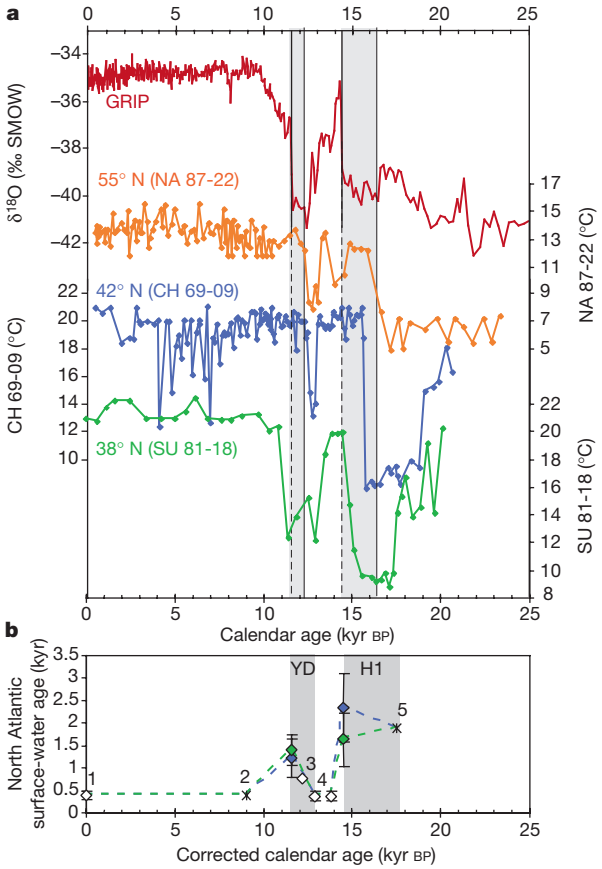

Figure 2 Surface temperature records and reconstructed evolution of the surface reservoir age during the last 18 kyr. **a**, Comparison of GRIP ice $\delta^{18}O$ (a proxy for air temperature) and summer SST reconstructions at the three North Atlantic sites versus calendar age. SST has been reconstructed from the planktonic foraminifera abundances by the revised analogue method[27,28]. Grey stripes highlight the large leads between NA 87-22 SST and GRIP air temperature at the H1–Bølling–Allerød and Younger Dryas–Holocene transitions. **b**, Tentative synthesis of variations in surface-water ages in the North Atlantic north of 40° N during the last 18 kyr. Filled diamonds, our results; unfilled diamonds, estimates available in the literature: 1, pre-bomb value[5,6]; 3, reservoir ages obtained by dating of the Vedde ash layer[7,8]; 4, Bølling–Allerød reservoir ages measured in Norwegian coastal waters[29]. Crosses, possible additional constraints: 2, ocean circulation in the North Atlantic can be considered as similar to today around 9 kyr BP (ref. 20); 5, approximate value derived from the difference between the initiation of the cooling associated with H1 in SU 81-18 and in CH 69-09, assuming a reservoir age of 0.4 kyr at the SU 81-18 site. Dotted line, proposed evolution of surface-water age at high latitudes in the North Atlantic.

of the northern $\delta^{18}O_b$ records with respect to the $\delta^{18}O_b$ signal of core SU 81-18. The lead of the northern records with respect to the mid-latitudes record seems thus to be an artefact of the ^{14}C chronology.

Second, no reasonable climatic mechanism can explain how SST at site NA 87-22, located in the same latitude band as Greenland, could have reached interglacial values 0.8–1.9 kyr before the SST off Portugal (site SU 81-18) and the air temperature above Greenland.

On the contrary, we have reasons to believe that the small surface-water ages currently observed in the North Atlantic did not prevail in the past. In fact, current constant reservoir ages over the North Atlantic are principally due to the North Atlantic Drift, which brings low-latitude surface waters to 50–60° N and into the Norwegian Sea. The cooling of warm and saline surface waters at high latitudes induces active deep-water formation in these areas, associated with a large flux of atmospheric ^{14}C to the surface waters. Consequently, the presence of large continental ice caps, the southward shift of the polar front and the associated shift in deep-water-formation areas during the Younger Dryas cold episode and the last glacial maximum[17–21] probably explain an important decrease in ventilation and hence an increase in surface-water reservoir age, north of the polar front[7]. It was also demonstrated that iceberg discharge H1 had a large impact on ocean circulation, further reducing NADW formation[20,22].

The effect of circulation changes on the ocean radiocarbon content has been evaluated with coupled ocean–ice–atmosphere models[23–25]. These modelling experiments show that a reduction in NADW overturn and an increase in sea ice cover lead to an increase in surface-water age of 200–300 yr in the Atlantic, north of 40° N. These results are thus consistent with our findings, although the increase in surface reservoir age predicted by the models is weaker than our data indicate. This seems to result from the fact that these models simulate no or very little vertical convection north of the polar front, although palaeoceanographic data show the opposite[26].

The two northernmost cores demonstrated leads of the SST abrupt warmings with respect to the air temperature increases recorded in the Greenland ice. We interpret these leads as increases in the surface reservoir age at the cores' location during these two specific climatic transitions. A tentative reconstruction of the evolution of the Atlantic surface-water age during the last 18 kyr can be derived from the compilation of available estimates of apparent surface-water ages (Fig. 2b). After correcting the marine time scales to account for these large reservoir ages, the three $\delta^{18}O_b$ records are in much better agreement between 11 and 18 kyr (Fig. 3b), the residual differences probably resulting from measurement uncertainties, noise due to bioturbation, and small differences in deep water temperature variations between sites.

This study allowed us to reconcile ice core and North Atlantic marine chronologies, as well as surface and deep-water climatic records from mid- to high latitudes, over the entire deglaciation period. We demonstrated that the surface-water age at high latitudes in the North Atlantic has varied by a factor of 3–5 during the past 15 kyr, owing presumably to major changes in ocean circulation and sea ice cover. It is therefore highly probable that it also significantly varied across the Heinrich and Dansgaard–Oeschger climatic events of the last glacial period (see for example ref. 2), inducing biases in marine ^{14}C chronologies. The situation at high southern latitudes is expected to be similar, as indicated by recent measurements showing large increases in surface reservoir ages in the New Zealand region during glacial times[10]. □

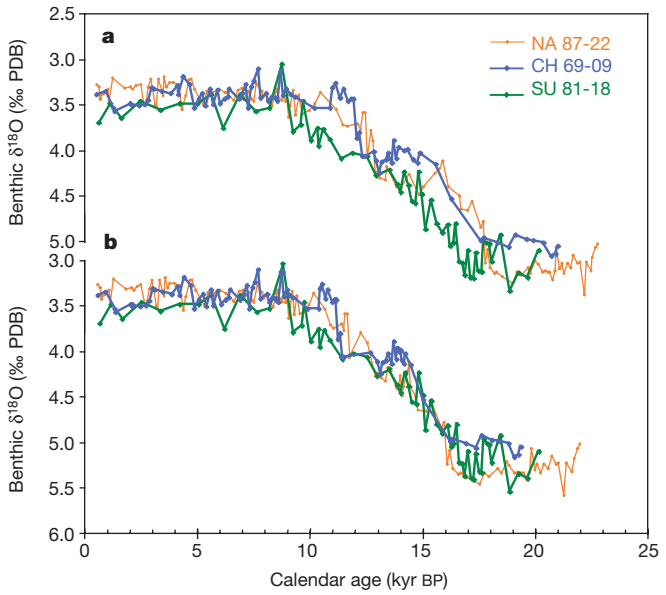

Figure 3 $\delta^{18}O_b$ records from the three North Atlantic cores. Data[11,12,30] are expressed in ‰ versus the Pee Dee Belemnite (PDB) standard. **a**, Records versus the calendar-age scale defined in Fig. 1. **b**, Same records after correcting the original age scale to account for the variations in surface-water age according to our tentative synthesis (Fig. 2b).

1. Bard, E. *et al.* Retreat velocity of the North Atlantic polar front during the last deglaciation determined by ^{14}C accelerator mass spectrometry. *Nature* **328,** 791–794 (1987).
2. Voelker, A. *et al.* Correlation of marine ^{14}C ages from the Nordic Seas with the GISP2 isotope record: Implications for ^{14}C calibration beyond 25 ka BP. *Radiocarbon* **40,** 517–534 (1998).
3. Stuiver, M. *et al.* INTCAL98 radiocarbon age calibration, 24,000-0 cal BP. *Radiocarbon* **40,** 1041–1083 (1998).
4. Alley, R. B. *et al.* Abrupt increase in Greenland snow accumulation at the end of the Younger Dryas event. *Nature* **362,** 527–529 (1993).
5. Bard, E. Correction of accelerator mass spectrometry ^{14}C ages measured in planktonic foraminifera: paleoceanographic implications. *Paleoceanography* **3,** 635–645 (1988).
6. Stuiver, M. & Braziunas, T. F. Sun, ocean, climate and atmospheric $^{14}CO_2$: an evaluation of causal and spectral relationship. *The Holocene* **3,** 289–305 (1993).
7. Bard, E. *et al.* The North Atlantic atmosphere-sea surface ^{14}C gradient during the Younger Dryas climatic event. *Earth Planet. Sci. Lett.* **126,** 275–287 (1994).
8. Austin, W. E. N., Bard, E., Hunt, J. B., Kroon, D. & Peacock, J. D. The ^{14}C age of the Icelandic Vedde Ash: implications for Younger Dryas marine reservoir age corrections. *Radiocarbon* **37,** 53–62 (1995).
9. Siani, G. *Estimation de l'âge ^{14}C du réservoir des eaux de surface de la mer Méditerranée pendant les derniers 18000 ans.* Thesis, Univ. Paris-Sud (1999).
10. Sikes, E. L., Samson, C. R., Guilderson, T. P. & Howard, W. R. Old radiocarbon ages in the southwest Pacific Ocean during the last glacial period and deglaciation. *Nature* **405,** 555–559 (2000).
11. Duplessy, J. C. *et al.* Changes in surface salinity of the North Atlantic Ocean during the last deglaciation. *Nature* **358,** 485–487 (1992).
12. Labeyrie, L. *et al.* in *Mechanisms of Global Climate Change at Millennial Time Scales, Geophysical Monograph Series 112* (eds Clark, P. & Webb, R. S.) 77–98 (American Geophysical Union, Washington, DC, 1999).
13. Stuiver, M. & Reimer, P. J. Extended ^{14}C data base and revised CALIB 3.0 ^{14}C age calibration program. *Radiocarbon* **35,** 215–230 (1993).
14. Bard, E., Arnold, M., Duprat, J., Moyes, J. & Duplessy, J. C. Reconstruction of the last deglaciation: deconvolved records of $\delta^{18}O$ profiles, micropaleontological variations and accelerator mass spectrometric ^{14}C dating. *Clim. Dynam.* **1,** 101–112 (1987).
15. Johnsen, S. J. *et al.* The $\delta^{18}O$ record along the Greenland Ice Core Project deep ice core and the problem of possible Eemian climatic instability. *J. Geophys. Res.* **102,** 26397–26410 (1997).
16. Broecker, W., Bond, G., Klas, M., Clark, E. & MacManus, J. Origin of the northern Atlantic's Heinrich events. *Clim. Dynam.* **6,** 265–273 (1992).
17. Boyle, E. A. Cadmium: chemical tracer deepwater paleoceanography. *Paleoceanography* **3,** 471–489 (1988).
18. Labeyrie, L. D. *et al.* Changes in vertical structure of the North Atlantic Ocean between glacial and modern times. *Quat. Sci. Rev.* **11,** 401–413 (1992).
19. Duplessy, J.-C. *et al.* Deepwater source variations during the last climatic cycle and their impact on the global deepwater circulation. *Paleoceanography* **3,** 343–360 (1988).
20. Sarnthein, M. *et al.* Changes in east Atlantic deepwater circulation over the last 30,000 years: eight time slice reconstructions. *Paleoceanography* **9,** 209–267 (1994).
21. Muscheler, R., Beer, J., Wagner, G. & Finkel, R. Changes in deep-water formation during the Younger Dryas event inferred from ^{10}Be and ^{14}C records. *Nature* **408,** 567–570 (2000).
22. Vidal, L. *et al.* Evidence for changes in the North Atlantic Deep Water linked to meltwater surges during the Heinrich events. *Earth Planet. Sci. Lett.* **146,** 13–26 (1997).
23. Mikolajewicz, U. A meltwater induced collapse of the conveyor belt thermohaline circulation and its influence on the distribution of $\Delta^{14}C$ and $\delta^{18}O$ in the oceans. *Max Planck Inst. Rep.* **189,** 1–25 (1996).
24. Stocker, T. F. & Wright, D. G. Rapid changes in ocean circulation and atmospheric radiocarbon. *Paleoceanography* **11,** 773–795 (1996).
25. Stocker, T. F. & Wright, D. G. The effect of a succession of ocean ventilation changes on ^{14}C. *Radiocarbon* **40,** 359–366 (1998).
26. Dokken, T. M. & Jansen, E. Rapid changes in the mechanism of ocean convection during the last glacial period. *Nature* **401,** 458–461 (1999).
27. Waelbroeck, C. *et al.* Improving past sea surface temperature estimates based on planktonic fossil faunas. *Paleoceanography* **13,** 272–283 (1998).

28. Malmgren, B., Kucera, M., Nyberg, J. & Waelbroeck, C. Comparison of available statistical and artificial neural network techniques for estimating past sea-surface temperatures from planktonic foraminifera census data. *Palaeoceanography* (in the press).
29. Bondevik, S., Birks, H. H., Gulliksen, S. & Mangerud, J. Late Weichselian marine ^{14}C reservoir ages at the western coast of Norway. *Quat. Res.* **52,** 104–114 (1999).
30. Labeyrie, L. *et al.* Surface and deep hydrology of the northern Atlantic Ocean during the last 150,000 years. *Phil. Trans. R. Soc. Lond.* **348,** 255–264 (1995).

Supplementary information is available on *Nature*'s World-Wide Web site (http://www.nature.com) or as paper copy from the London editorial office of *Nature*.

Acknowledgements

We thank E. Bard and G. Siani for discussions and comments. The data were acquired in collaboration with T. van Weering, J.-L. Turon, M. Labracherie and G. Auffret. We thank B. Lecoat and J. Tessier for processing the isotopic measurements. This study was supported by CNRS, CEA, INSU (PNEDC) and EU Environment Program.

Correspondence and requests for materials should be addressed to C.W. (e-mail: Claire.Waelbroeck@lsce.cnrs-gif.fr).

Direct observation of a submarine volcanic eruption from a sea-floor instrument caught in a lava flow

Christopher G. Fox*†, William W. Chadwick Jr†‡ & Robert W. Embley*

* *NOAA/PMEL, Newport, Oregon 97365, USA*
‡ *2115 SE OSU Drive, Oregon State University/NOAA, Newport, Oregon 97365, USA*
† *These authors contributed equally to this work*

Our understanding of submarine volcanic eruptions has improved substantially in the past decade owing to the recent ability to remotely detect such events[1] and to then respond rapidly with synoptic surveys and sampling at the eruption site. But these data are necessarily limited to observations after the event[2]. In contrast, the 1998 eruption of Axial volcano on the Juan de Fuca ridge[3,4] was monitored by *in situ* sea-floor instruments[5–7]. One of these instruments, which measured bottom pressure as a proxy for vertical deformation of the sea floor, was overrun and entrapped by the 1998 lava flow. The instrument survived—being insulated from the molten lava by the solidified crust—and was later recovered. The data serendipitously recorded by this instrument reveal the duration, character and effusion rate of a sheet flow eruption on a mid-ocean ridge, and document over three metres of lava-flow inflation and subsequent drain-back. After the brief two-hour eruption, the instrument also measured gradual subsidence of 1.4 metres over the next several days, reflecting deflation of the entire volcano summit as magma moved into the adjacent rift zone. These findings are consistent with our understanding of submarine lava effusion, as previously inferred from seafloor observations, terrestrial analogues, and laboratory simulations[8–11].

Two Volcanic System Monitor (VSM) instruments were deployed at Axial volcano in October 1997, one near the centre of the caldera[5] and one on the upper south rift zone, hereafter referred to as VSM1 and VSM2, respectively (Figs 1 and 2). The VSM instruments measure ambient pressure on the sea floor every 15 s with a Paroscientific digiquartz pressure sensor. The data processing methods are described in detail elsewhere[5,12], but include filtering to remove oceanographic phenomena and a correction for temperature. In August 1998, VSM2 was found to be trapped in the new lava flow (Fig. 1), but it was pulled free the following summer.

The rescued instrument was in surprisingly good condition. The maximum temperature recorded inside VSM2 during the eruption was only 7.5 °C (Fig. 3)—remarkably low, considering that the instrument was sitting atop basaltic lava that was probably erupted at ~1,190 °C (M. Perfit, personal communication). This was apparently due to the thermal insulation provided by the surface crust that forms (and quickly thickens) when submarine lava flows come into contact with frigid sea water[13].

The northern end of the 1998 lava flow where VSM2 was located (Fig. 2) is a long, narrow sheet flow[4]. Submarine sheet flows are thought to form by brief, relatively high-effusion-rate eruptions[8,9]. Recent models[10,11] suggest that such flows initially advance as thin lobate flows (20–30 cm thick), spreading at a rate that is rapid enough for the interior of the flow to remain a single fluid core beneath a solid upper crust. The flow spreads until it becomes laterally confined, and then 'inflates' upward. During inflation, the upper crust is uplifted (sometimes > 5 m) by hydraulic pressure within the flow interior—and lava pillars grow upward, connecting the upper and lower crusts[10]. Lava inflation continues until the eruption rate wanes or stops, at which point lava begins to drain back and the upper crust founders where it is left unsupported, leaving extensive areas of collapse within the flow.

Geologic mapping of the 1998 lava flow shows that VSM2 was located in the collapsed interior of the 1998 lava flow, ~3 m below nearby remnants of the uncollapsed upper crust and ~160 m west of the eruptive fissure (Fig. 2). The instrument had not been buried by lava, even though the lava level had been 3 m higher before collapse. This observation implies that lava initially flowed under the instrument, which became embedded in the upper crust of the flow when the flow subsequently inflated. During inflation, VSM2 was uplifted along with the upper crust (because of its table-like design) and then was set back down within the collapse area during the drain-back stage.

The dataset recovered from the VSM2 instrument directly recorded this sequence of events (Fig. 3). Uplift of the instrument began slowly at 14:55 on 25 January 1998 (all times GMT), after the onset of the earthquake swarm at 11:33 (ref. 3) and subsidence began at VSM1 at 14:51 (ref. 5). Rapid inflation abruptly started at 15:16 when VSM2 was uplifted 168 cm in the next 5 minutes, an average rate of 32 cm min^{-1} (although instantaneous rates were as high as 73 cm min^{-1}). After a pause of 4 minutes, during which the instrument subsided 13 cm, inflation resumed for another 21 minutes which uplifted the instrument another 113 cm at a decreased rate of 5.5 cm min^{-1}. At 15:46, inflation dramatically slowed, probably owing to a sudden reduction in the effusion rate at the vent, and the instrument was only uplifted another 7 cm over the next 21 minutes. During this period the lava flow remained at or near its fully inflated thickness, and the recorded temperature reached its peak of 7.5 °C at 15:49 (Fig. 3).

At this point, lava inflation ended and lava drain-back began, presumably reflecting the end of lava effusion at the vent. Our

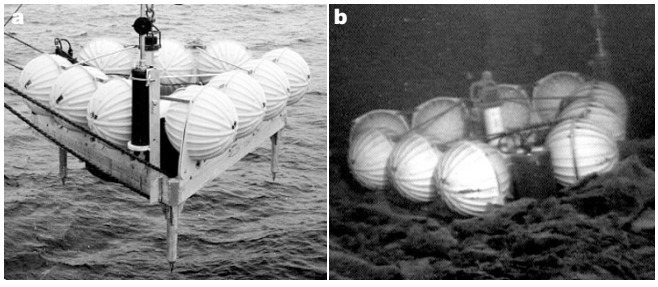

Figure 1 Views of the VSM2 instrument. **a**, At the surface during deployment (legs are 46 cm long), and **b**, on the sea floor, stuck in the 1998 lava flow at Axial volcano. Virtual animations and video clips of VSM2 (referred to as a 'rumbleometer') on the sea floor are available at http://www.pmel. noaa.gov/vents/nemo/explorer/rumble.html

Acknowledgements

We acknowledge financial support of the Deutsche Forschungsgemeinschaft and of Roche Diagnostics. P. Göttig and R. Ramachandran helped with biochemical analyses. We thank G. Bourenkov and H. Bartunik, and G. Leonard for help with synchrotron data collection at DESY BW6 (Hamburg) and ESRF ID14-4 (Grenoble), respectively.

Competing interests statement

The authors declare that they have no competing financial interests.

Correspondence should be addressed to H.B. (e-mail: hbs@biochem.mpg.de). The coordinates of the tricorn protease have been deposited in Protein Data Bank under accession code 1K32.

addendum

An efficient room-temperature silicon-based light-emitting diode

Wai Lek Ng, M. A. Lourenço, R. M. Gwilliam, S. Ledain, G. Shao & K. P. Homewood

Nature **410,** 192–194 (2001).

Silicon light-emitting diodes (LED) show light emission at the bandgap energy of silicon with efficiencies approaching those of standard III–V emitters: 0.1% for planar devices (our Letter) and about 1% when total internal reflection is minimized by surface texturing[1]. We point out here an additional example of a silicon device also showing light emission at the bandgap[2]. The authors described devices made by the SACMOS-3 process and focus the bulk of the paper on visible emission under reverse bias. However, they also report briefly on a device operated under forward bias giving efficiencies of around 0.01%, although no explanation of the mechanism is given. It is now becoming clear that crystalline silicon, when appropriately engineered, is capable of supporting efficient light emission, opening up many significant applications. □

1. Green, M. A., Shao, J., Wang, A., Reece, P. J. & Gal, M. Efficient silicon light-emitting diodes. *Nature* **412,** 805–808 (2001).
2. Kramer, J. *et al.* Light-emitting devices in industrial CMOS technology. *Sensors Actuators* **A37–A38,** 527–533 (1993).

erratum

Warm tropical sea surface temperatures in the Late Cretaceous and Eocene epochs

Paul N. Pearson, Peter W. Ditchfield, Joyce Singano, Katherine G. Harcourt-Brown, Christopher J. Nicholas, Richard K. Olsson, Nicholas J. Shackleton & Mike A. Hall

Nature **413,** 481–487 (2001).

In this Article, the temperature scale in Figure 3i should have been the same as in Figure 3g. □

corrections

Self-assembled monolayer organic field-effect transistors

Jan Hendrik Schön, Hong Meng & Zhenan Bao

Nature **413,** 713–716 (2001).

The values of the transconductance in Table 1 and in the text (page 715, second paragraph) are incorrect. The values should be divided by ten. The data plotted in Figs 2 and 3 are correct and the conclusions are not affected. □

Ordered nanoporous arrays of carbon supporting high dispersions of platinum nanoparticles

Sang Hoon Joo, Seong Jae Choi, Ilwhan Oh, Juhyoun Kwak, Zheng Liu, Osamu Terasaki & Ryong Ryoo

Nature **412,** 169–172 (2001).

We inadvertently omitted to cite an earlier reference alongside ref. 8 (G. Che, B. Lakshmi, E. R. Fisher and C. R. Martin *Nature* **393,** 346–349; 1998), which was published in 1995 (and not 2000 as printed). Also, our suggestion that using the pores in a microporous material as templates could be a way in which to produce nanoscale materials has been discussed before (see, for example, C. R. Martin *Science* **266,** 1961–1966 (1994) and J. C. Hulteen & C. R. Martin *J. Mater. Chem.* **7,** 1075–1087 (1997)). □

The timing of the last deglaciation in North Atlantic climate records

Claire Waelbroeck, Jean-Claude Duplessy, Elisabeth Michel, Laurent Labeyrie, Didier Paillard & Josette Duprat

Nature **412,** 724–727 (2001).

We directly used the observed leads of sea surface temperature with respect to air temperature (dated in calendar years), whereas the air temperature calendar ages should have been converted into ^{14}C ages, with reservoir ages computed as the difference between marine and atmospheric ^{14}C ages. Taking this into consideration, apparent surface-water ages are 1,180 ± 630 to 1,880 ± 750 years at the end of the Heinrich 1 surge event (14,500 years BP) and 930 ± 250 to 1,050 ± 230 years at the end of the Younger Dryas cold episode. This does not change the discussion and conclusions. □